Journal of Applied Mathematics and Physics (ZAMP)
Vol. 42, January 1991

0044-2275/91/010122-17 $ 1.50 + 0.20

Locally forced critical surface waves in channels of arbitrary cross section

By S. S. P. Shen, Dept of Mathematics, University of Saskatchewan, Saskatoon, Saskatchewan, Canada S7N 0W0

1. Introduction

We consider long near critical surface waves forced by locally distributed pressure applied on the free surface in channels of arbitrary cross section. The fluid under consideration is inviscid and has constant density. The upstream flow is uniform and the upstream velocity is near critical, i.e., $u_0 = u_c + \varepsilon\lambda + 0(\varepsilon^2)$, where u_c is the critical velocity and $0 < \varepsilon \ll 1$. The external pressure applied on the free surface is $\varepsilon^2 P\delta(x)$, where $\delta(x)$ is the Dirac delta function. This forcing is equivalent to having a localized bottom topography whose amplitude is of order ε^2 and that varies along the longitudinal direction of the channel.

The study of such forced nonlinear free surface waves has attracted many researchers' attention recently. Since 1982, there has been a vast amount of research work published on this subject. Most experimental and numerical work has been done on two-dimensional channels (Wu and Wu [1], Forbes and Schwartz [2], Vanden-Broeck [3], and Forbes [4], etc.). Asymptotic approximation method has also been used to study this problem by Akylas [5], Cole [6], Miles [7], Mei [8], Wu [9], Shen [10–11], and others. Two dimensional and three dimensional waves in a rectangular channel were studied by Mei [8] and Ertekin et al. [12] respectively. Two dimensional waves in channels of arbitrary cross section were studied in [10–11]. We may summarize their results as follows:

(i) There exist two supercritical stationary solitary waves;
(ii) There exists one subcritical downstream cnoidal wave;
(iii) There exists one hydraulic fall which transmits an upstream subcritical flow to a downstream supercritical flow;
(iv) There exist no transcritical steady state waves;
(v) At some upstream transcritical velocities, solitons are periodically generated at the location of the forcing and radiated upstream.

For a two-dimensional channel, Miles showed (iv) analytically *via* Rayleigh asymptotic reduction process [7]. He assumed that the external forcing is localized (he called it *compact*). With this assumption, he was able to express the forcing in the asymptotically reduced equation in terms of the Dirac delta function. Then he found the exact Froude number range (F_L, F_C), in which no steady state free surface waves exist. He also mentioned in [7] that there possibly exist two solitary wave solutions when the Froude number $F > F_c$. Nonetheless, he did not explicitly find them. This nonuniqueness of stationary solitary wave solutions for an $fK-dV$ was first noticed by Patone and Warn as early as 1982 for a special type of forcing [13], and was later systematically studied in [10].

In this paper, we adopt Miles' assumption of localized forcing. The forced Korteweg–de Vries equation $fK-dV$ derived by Shen [10–11] is used as our model equation. The assumption of localized forcing enables us to find solutions of an $fK-dV$ analytically. In this paper we focus on steady state solutions. An initial work on finding unsteady state analytic solutions of an $fK-dV$ can be found in [14]. In section 2, we recapitulate the derivation of $fK-dV$. In section 3, we find $\lambda_c = (3b^2P^2\alpha^2/(-4\beta m_1^2))^{1/3}$ analytically and show that there are two cusped solitary waves for each $\lambda > \lambda_c$. It is also found that when $\lambda = \lambda_d = (3\alpha^2 b^2 P^2/(-\beta m_1^2))^{1/3}$, there exists a jump solution, which consists of a horizontal free surface downstream matched with a semi-solitary wave upstream. The difference between the downstream larger depth and the upstream smaller depth is $-\lambda_d/\alpha$. In section 4, we find $\lambda_L = (3b^2P^2\alpha^2/\beta m_1^2)^{1/3} = -\lambda_d$ analytically and show that there is unique downstream cnoidal wave solution matched with the upstream null solution when $\lambda < \lambda_L$. It is also shown that there is a unique wave free hydraulic fall solution when $\lambda = \lambda_L$. In this steady state, the upstream flow is subcritical and the downstream flow is supercritical.

The difference between this paper and my previous work [10, 11] is that here analytic solutions of the $fK-dV$ equation, which before required numerical solutions, are found because of the assumption of localized forcing. Thus many of the previous results become more transparent. The results obtained here are consistent with those of [10, 11]. It appears that such an approach to study surface waves in channels of arbitrary cross section is novel.

2. A forced Korteweg–de Vries equation

Consider an inviscid fluid flow in a channel of arbitrary but uniform cross section. Let L and H be longitudinal and transverse length scales of the flow respectively. The x^*-axis is aligned along the longitudinal direction of the channel, the y^*-axis along the spanwise direction and the z^*-axis vertically in the opposite direction to gravitation. The x^*, y^* plane is placed on the upstream undisturbed free surface. The equation of the boundary of the channel is $h^*(y^*, z^*) = 0$. The equation of the free surface is $z^* = \eta^*(x^*, y^*, t^*)$, where t^* is time coordinate. (u^*, v^*, w^*) is velocity; ϱ^* is density; p^* is pressure; g is the gravitational acceleration constant; and $\bar{p}^*$ which is assumed to be function of x^* only, is the external pressure applied on the free surface. The superscript $*$ signifies dimensional quantities.

The following dimensionless quantities are introduced:

$$\varepsilon = \left(\frac{H}{L}\right)^2 \ll 1, \quad t = \varepsilon^{3/2}\sqrt{\frac{g}{H}}\,t^*,$$

$$(x, y, z) = \frac{1}{H}(\varepsilon^{1/2}x^*, y^*, z^*),$$

$$\eta = \frac{\eta^*}{H}, \quad p = \frac{p^*}{\varrho^* gH}, \quad \bar{p} = \varepsilon^2\frac{\bar{p}^*}{\varrho gH},$$

$$(u, v, w) = \frac{1}{\sqrt{gH}}(u^*, \varepsilon^{-1/2}v^*, \varepsilon^{-1/2}w^*),$$

$$h_2 = h^*_{y^*}, \quad h_3 = h^*_{z^*}.$$

In the following, we adopt three basic asymptotic assumptions:

(i) The upstream velocity is near critical, i.e.

$$u_0 = u_c + \varepsilon\lambda + O(\varepsilon^2); \tag{1}$$

(ii) The amplitude of the applied external pressure on the free surface is of order $O(\varepsilon^2)$, i.e. $\bar{p} = \varepsilon^2\bar{p}^*/(\varrho^* gH)$;

(iii) The amplitude of the free surface elevation is of order $O(\varepsilon)$, i.e.,

$$\eta = \varepsilon\eta_1(x, t) + \varepsilon^2\eta_2(x, y, t) + O(\varepsilon^3). \tag{2}$$

Then it can be shown (see [10] or [11]) that:

(A) The critical velocity u_c satisfies

$$u_c^2 = \frac{A}{b} \tag{3}$$

where A is the wet area of cross section of the channel and b is width of the channel (see Figure 1);

(B) The first order perturbation of the free surface η_1 satisfies a forced Korteweg–de Vries equation (fK–dV)

$$m_1\eta_{1t} + \lambda m_1\eta_{1x} + m_2\eta_1\eta_{1x} + m_3\eta_{1xxx} = -f(x), \tag{4}$$

where

$$m_1 = -2b\sqrt{b/A}, \tag{5}$$

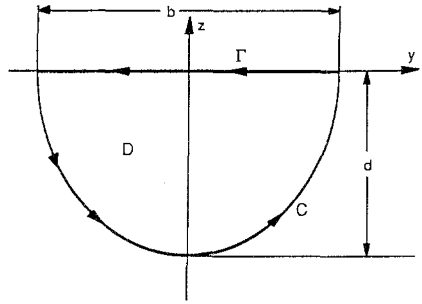

Figure 1
D is the wet area of the cross section of a channel (also see equations (7) and (9)).

$$m_2 = 3b^2/A - (b/A) \int_\Gamma \phi_{yy}\, dy, \tag{6}$$

$$m_3 = (b/A) \int_D \int |\nabla\phi|^2\, dy\, dz, \tag{7}$$

$$f(x) = b\bar{p}_x. \tag{8}$$

In (4)–(8), the integration domain D and the integration contour Γ are shown in Figure 1. $\nabla = (\partial/\partial y, \partial/\partial x)$, and $\phi = \phi(y, z)$ is a solution of the following Neumann problem:

$$\nabla^2\phi = 1 \quad \text{in } D, \tag{9}$$

$$\phi_z = \frac{A}{b} \quad \text{on } \Gamma, \tag{10}$$

$$\phi_n = 0 \quad \text{on } C \tag{11}$$

where $\nabla^2 = (\partial^2/\partial y^2) + (\partial^2/\partial x^2)$ and ϕ_n is the unit outward normal derivative of ϕ on C.

The details of the derivation of (3)–(11) can be found in [10] or [11]. From (4)–(11), we see that the coefficients m_1, m_2 and m_3 of the fK–dV (4) are entirely determined by the geometry of the cross section of the channel. The upstream velocity enters the fK–dV only by λ. It is this λ that controls the behavior of the solutions of the fK–dV. For different values of λ, the solutions of the fK–dV may be dramatically different. We may see this in section 3–5.

If D is a rectangle or a triangle, m_1, m_2 and m_3 can be found very easily [10]. If D is an ellipse, a conformal mapping method can be used to find m_1, m_2 and m_3 (Cai and Shen [18]). For the data used in this paper, see Table 1.

When the forcing is localized, then $\bar{p}(x) = P\delta(x)$, where $\delta(x)$ is the Dirac delta function. Physically, it means that if the support of $\bar{p}(x)$ is very small compared with the wave length which measured by L, then the distributed

Table 1
Bifurcation data for rectangular, triangular and elliptic channels.

	b	d	m_1	m_2	m_3	α	β	P	λ_C	λ_L	λ_d
Rectangular	1	1	-2	3	$\frac{1}{3}$	$-\frac{3}{4}$	$-\frac{1}{6}$	1	0.859	-1.36	1.36
Triangular	1	1	$-2^{3/2}$	5	$\frac{13}{48}$	$-\frac{5\ 2^{1/2}}{8}$	$-\frac{13\ 2^{1/2}}{192}$	1	0.914	-1.45	1.45
Elliptic	2	1	$-\frac{8}{\pi^{1/2}}$	$\frac{48}{\pi^{3/2}}$	0.666	$-\frac{3}{\pi}$	-0.15	1	0.970	-1.54	1.54

pressure applied on the free surface may be considered approximately as a concentrated force of magnitude P. In the following we only study the case of localized forcing.

3. Supercritical steady flow: solitary waves

For a steady state flow, the fK–dV (4) becomes

$$\lambda\eta_{1x} + 2\alpha\eta_1\eta_{1x} + \beta\eta_{1xxx} = -\frac{b}{m_1}\bar{p}_x, \quad \lambda > 0 \tag{12}$$

where $\alpha = m_2/(2m_1)$ and $\beta = m_3/m_1$. Since the upstream flow is uniform, we have

$$\eta_1(-\infty) = \eta_{1x}(-\infty) = \eta_{1xx}(-\infty) = 0. \tag{13}$$

Using $\bar{p} = P\delta(x)$, the first integral of (12) reads

$$\lambda\eta_1 + \alpha\eta_1^2 + \beta\eta_{1xx} = -\frac{b}{m_1}P\delta(x), \quad \lambda > 0. \tag{14}$$

We look for solitary wave solutions of (14). Hence η_1 satisfies the boundary conditions:

$$\eta_1(\pm\infty) = \eta_{1x}(\pm\infty) = 0. \tag{15}$$

By direct integration, the solutions of (14)–(15) can be expressed as follows

$$\eta_1(x) = -\frac{3\lambda}{2\alpha}\operatorname{sech}^2\sqrt{\frac{-\lambda}{4\beta}}(x - L_+), \quad x > 0, \tag{16}$$

$$\eta_1(x) = -\frac{3\lambda}{2\alpha}\operatorname{sech}^2\sqrt{\frac{-\lambda}{4\beta}}(x - L_-), \quad x < 0 \tag{17}$$

where L_+ and L_- are constants. The continuity condition of the free surface at $x = 0$

$$\eta_1(0+) = \eta_1(0-) \equiv \eta_1(0)$$

implies that

$$L_+ = \pm L_-. \tag{18}$$

Because of $\delta(x)$ in (14), η_{1x} must have a jump discontinuity at $x = 0$. Namely,

$$\eta_{1x}(0+) - \eta_{1x}(0-) = -\frac{bP}{\beta m_1}.$$

By (16) and (17), this condition can be written as

$$-\sqrt{\frac{-\lambda}{\beta}}\,\eta_1(0)\left[-\tanh\left(\sqrt{\frac{-\lambda}{4\beta}}\,L_+\right) + \tanh\left(\sqrt{\frac{-\lambda}{4\beta}}\,L_-\right)\right] = -\frac{bP}{\beta m_1}. \tag{19}$$

This equation holds for a nonzero P only if $L_+ \neq L_-$, and by (18),

$$L_+ = -L_- = L_0.$$

Hence (19) can be written as

$$f^3 - f - c = 0 \tag{20}$$

where

$$f = \tanh\left(\sqrt{\frac{-\lambda}{4\beta}}\,L_0\right), \tag{21}$$

$$c = \frac{bP\alpha}{3m_1\lambda}\frac{1}{\sqrt{-\beta\lambda}}. \tag{22}$$

By $f^3 - f = f(f+1)(f-1)$, we see that

(i) when $|c| < 2/(3\sqrt{3})$, (20) has three distinct real roots and only two of them are in $(-1, 1)$;

(ii) when $|c| > 2/(3\sqrt{3})$, (20) has only one real root whose absolute value is greater than one;

(iii) when $|c| = 2/(3\sqrt{3})$, (20) has a double real root whose absolute value is less than one and the third real root is not in $(-1, 1)$.

So

$$c = \frac{bP\alpha}{3m_1\lambda}\frac{1}{\sqrt{-\beta\lambda}} = \pm\frac{2}{3\sqrt{3}}$$

determines the critical value of λ:

$$\lambda_c = \left(\frac{3b^2P^2\alpha^2}{-4m_1^2\beta}\right)^{1/3}. \tag{23}$$

Therefore

$$L_0 = \sqrt{\frac{4\beta}{-\lambda}}\,\operatorname{arctanh}(f) \tag{24}$$

has: (i) two solutions if $\lambda > \lambda_c$; (ii) one solution if $\lambda = \lambda_c$; and (iii) no solution if $0 \le \lambda < \lambda_c$. As soon as one finds L_0, the solution (16)–(17) is determined.

$$\eta_1(x) = -\frac{3\lambda}{2\alpha}\begin{cases}\operatorname{sech}^2\sqrt{\dfrac{-\lambda}{4\beta}}\,(x - L_0), & x \ge 0,\\[2ex] \operatorname{sech}^2\sqrt{\dfrac{-\lambda}{4\beta}}\,(x + L_0), & x \le 0.\end{cases} \tag{25}$$

For a given L_0, (25) defines a cusped solitary wave (see Figure 2c) and d)). The cusp is concave up (down) if $L_0 > 0$ (<0 respectively). By (20)–(22) and (24), we have:

$P < 0 \Rightarrow c < 0 \Rightarrow f > 0 \Rightarrow L_0 > 0 \Rightarrow$ cusp is concave up

$P > 0 \Rightarrow c > 0 \Rightarrow f < 0 \Rightarrow L_0 < 0 \Rightarrow$ cusp is concave down

Hence

$\operatorname{sign}(P) = -\operatorname{sign}(L_0)$.

Some solutions of (14)–(15), determined by (25), are shown in Figures 2c), d), for a triangular channel. Correspondingly, the saddle node bifurcation diagrams are shown in Figure 2a). The relationship between L_0 and λ is also shown in Figure 2b). The turning points of the bifurcation diagrams are computed from equation (23). For the bifurcation data, see Figure 2 a) and also see Table 1.

When $P > 0$, $\|\eta_1\|_\infty = -\dfrac{3\lambda}{2\alpha}\operatorname{sech}^2\!\left(\sqrt{\dfrac{-\lambda}{4\beta}}\,L_0\right) < -\dfrac{3\lambda}{2\alpha}$, which is the amplitude of the free solitary wave. The bifurcation diagram $\|\eta_1\|_\infty$ versus λ is given by

$$\|\eta_1\|_\infty = \frac{bP}{4m_1}\sqrt{\frac{-3}{\beta\lambda}}\left(\cos\left[\frac{1}{3}\arccos\left(\frac{\sqrt{3}bP\alpha}{2m_1\sqrt{-\beta\lambda^3}}\right) + \begin{Bmatrix}4\pi/3\\ 2\pi/3\end{Bmatrix}\right]\right)^{-1} \tag{26}$$

The $\|\eta_1\|_\infty - \lambda$ curve defined above has two branches. The upper branch and the lower branch correspond to $4\pi/3$ and $2\pi/3$ respectively in the above formula. The two branches are joined at λ_c, at which $\|\eta_1\|_\infty = -\lambda_c/\alpha$. As $P \to 0+$, $L_{01} \to 0-$ and $L_{02} \to -\infty$. Hence $\|\eta_1\|_\infty$ approaches $-3\lambda/2\alpha$ and zero respectively. See Fig. 2a).

When $P < 0$, $\|\eta_1\|_\infty = -3\lambda/2\alpha$ all the time. The cusped solitary waves have two peaks in each single solution. As $P \to 0-$, the two peaks of a

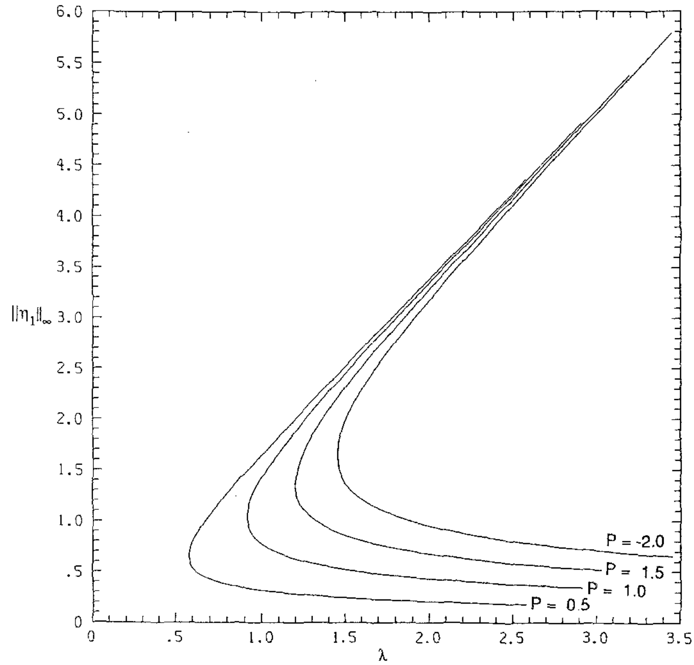

Figure 2 (a)

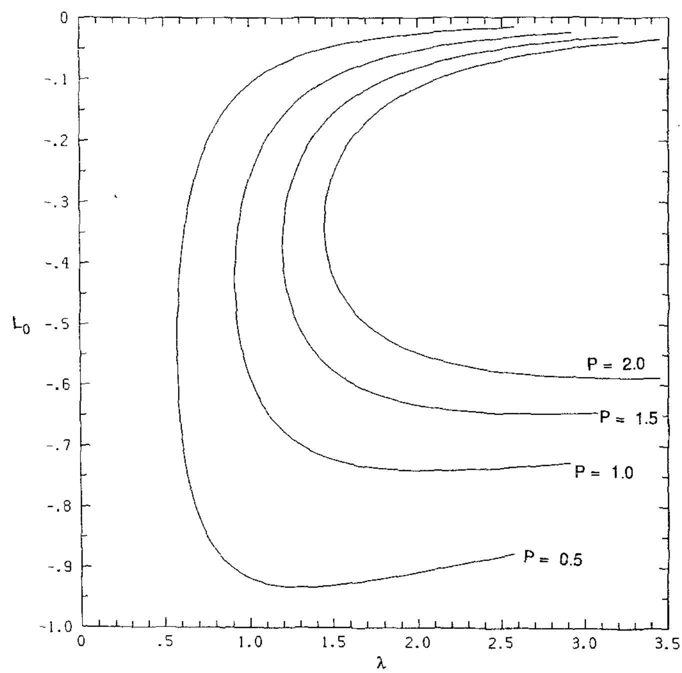

Figure 2 (b)

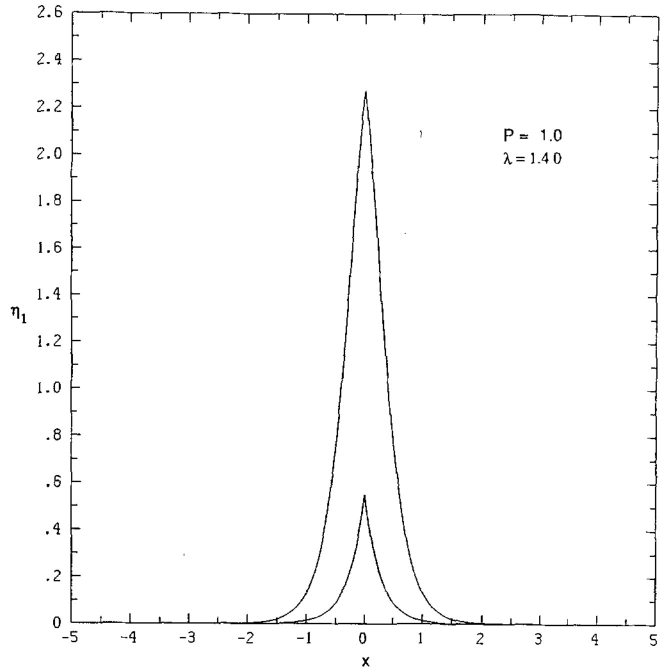

Figure 2(c)

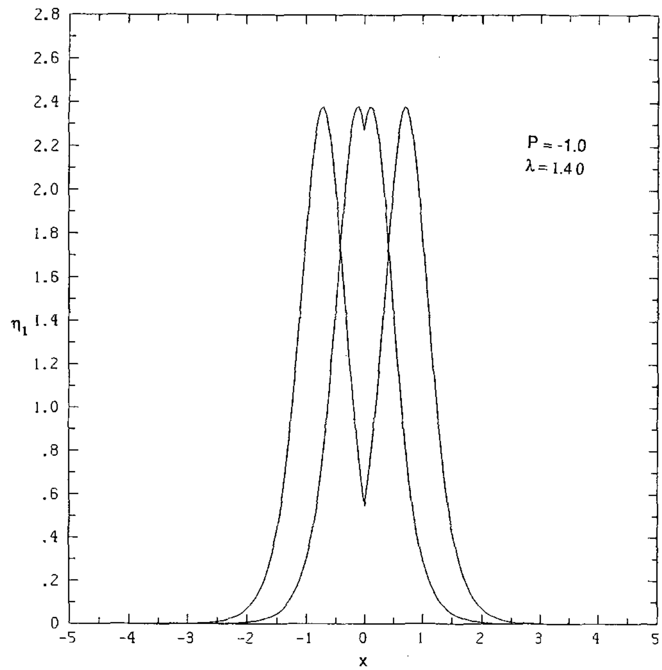

Figure 2(d)

Figure 2

Flows in a triangular channel: $b = d = 1$, $\alpha = -\dfrac{5\sqrt{2}}{8}$, $\beta = -\dfrac{13\sqrt{2}}{192}$. a) Bifurcation diagrams: $\lambda_c = 0.58$, 0.91, 1.2 and 1.45 when $P = 0.5$, 1.0, 1.5 and 2.0 respectively. b) Relationship between the phase shift L_0 and λ (see equation (24)). c) Two cusped solitary wave solutions of (14): $P = 1.0$, $\lambda = 1.4$, $L_{01} = -0.11$, $L_{02} = -0.71$. d) Two cusped solitary wave solutions of (14): $P = -1.0$, $\lambda = 1.4$, $L_{01} = 0.11$, $L_{02} = 0.71$.

cusped solitary wave merges and the cusp disappears gradually. The limit is the usual solitary wave in the case of no forcing. At the same time, the two peaks of the other cusped solitary wave move further apart to upstream and downstream respectively. The limit is the usual null solution in the case of no forcing since the peaks have moved to negative and positive infinities.

From $\operatorname{sign}(P) = -\operatorname{sign}(L_0)$, and from equation (25) which determines the free surface profile, we see that if $P < 0\,(>0)$, then the cusps of the solitary waves are concave up (down respectively). Namely, a surface suction ($P < 0$) corresponds to a dent of the free surface and a surface pressure ($P > 0$ corresponds to a crest of the free surface. This is consistent with the result obtained in [7], but is not consistent with one's intuition, and so it is a paradox.

Another supercritical wave free flow satisfies the following:

$$\lambda\eta_1 + \alpha\eta_1^2 + \beta\eta_{1xx} = -\frac{bP}{m_1}\delta(x), \quad \lambda > 0 \tag{27}$$

$$\eta_1(-\infty) = \eta_{1x}(-\infty) = 0, \quad \eta_1(+\infty) = \text{constant} > 0. \tag{28}$$

The unique solution of (27)–(28) can be expressed in the form

$$\eta_1(x) = \begin{cases} -\dfrac{3\lambda}{2\alpha}\operatorname{sech}^2\sqrt{\dfrac{-\lambda}{4\beta}}(x - x_0), & x < 0 \\ -\dfrac{\lambda}{\alpha} > 0, & x > 0. \end{cases} \tag{29}$$

This solution exists only for a special value of λ, called λ_d. λ_d and the phase shift x_0 are determined by the continuity condition of η_1 and the jump discontinuity condition of η_{1x} at $x = 0$:

$$\eta_1(0-) = -\frac{\lambda}{\alpha}, \quad \eta_{1x}(0-) = \frac{bP}{\beta m_1}.$$

By (29),

$$\tanh\left(\sqrt{\frac{-\lambda}{4\beta}}\,x_0\right) = \frac{\alpha P b}{m_1(-\beta\lambda^3)^{1/2}}. \tag{30}$$

By $\eta_1(0-) = -\lambda/\alpha$,

$$-\frac{3\lambda}{2\alpha}\left[1 - \tanh^2\left(\sqrt{\frac{-\lambda}{4\beta}}\,x_0\right)\right] = \lambda/\alpha. \tag{31}$$

Equations (30)–(31) imply

$$\lambda_d = \left(\frac{3\alpha^2 b^2 P^2}{-\beta m_1^2}\right)^{1/3} > 0. \tag{32}$$

Comparing (32) with (41), one sees that

$$\lambda_d > \lambda_c.$$

So the upstream velocity needed for the jump solution (29) to exist is larger than the minimum velocity needed for the solitary waves to exist. For solution profiles, see Figure 3. For a given forcing P and the geometry of the channel, the jump solution (29) exists only when $\lambda = \lambda_d$.

Next we show that for solution (29), the downstream flow is subcritical in the case of a square channel where $\alpha = -\frac{3}{4}$. The downstream Froude number can be approximately computed for the case of two dimensional channel flow. Let u_D be the dimensionless downstream velocity and $H_D = (1 - \varepsilon\lambda_d/\alpha)H$ be the downstream depth. Then the conservation of flux gives

$$(1 + \varepsilon\lambda_d)\sqrt{gH}H = u_D\sqrt{gH}H_D.$$

Hence

$$u_D = (1 + \varepsilon\lambda_d)\frac{H}{H_D}.$$

The downstream Froude number

$$\begin{aligned} F_D &= \frac{u_D\sqrt{gH}}{\sqrt{gH_D}} \\ &= (1 + \varepsilon\lambda_d)\left(1 - \varepsilon\frac{\lambda_d}{\alpha}\right)^{-3/2} \\ &= 1 - \varepsilon\lambda_d + 0(\varepsilon^2) < 1 \ \text{(subcritical)}. \end{aligned}$$

We need to point out that this transition from upstream lower surface level to downstream higher surface level is different from the well known hydraulic jump phenomenon (Yih [17]). Here the entire flow field is laminar and the mechanical energy is conservative. But in the case of a hydraulic jump, some mechanical energy is transformed to internal energy and the transition region is turbulent. In fact, this jump solution is a mirror image of the hydraulic fall which will be discussed in the next section.

4. Subcritical steady flow: cnoidal waves and hydraulic fall

Model equations in this section are (see equation (12)):

$$\lambda\eta_1 + \alpha\eta_1^2 + \beta\eta_{1xx} = -\frac{bP}{m_1}\delta(x), \quad \lambda < 0, \tag{33}$$

$$\eta_1(-\infty) = \eta_{1x}(-\infty) = 0. \tag{34}$$

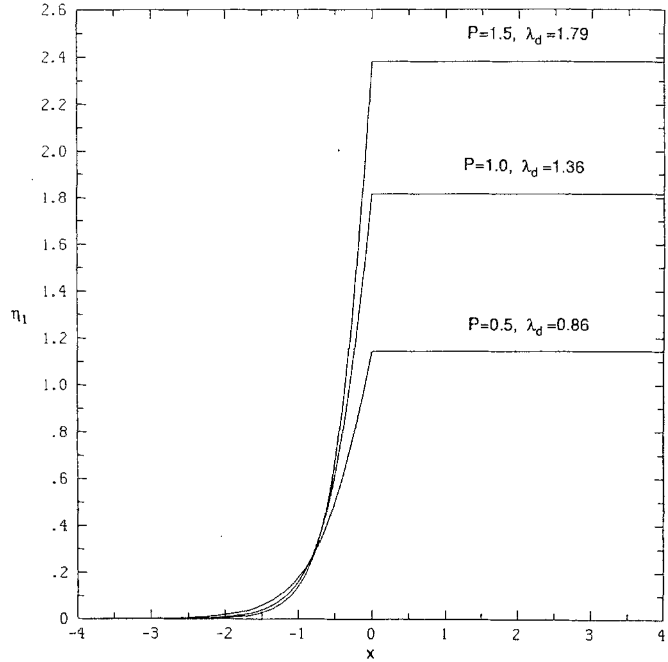

Figure 3(a)

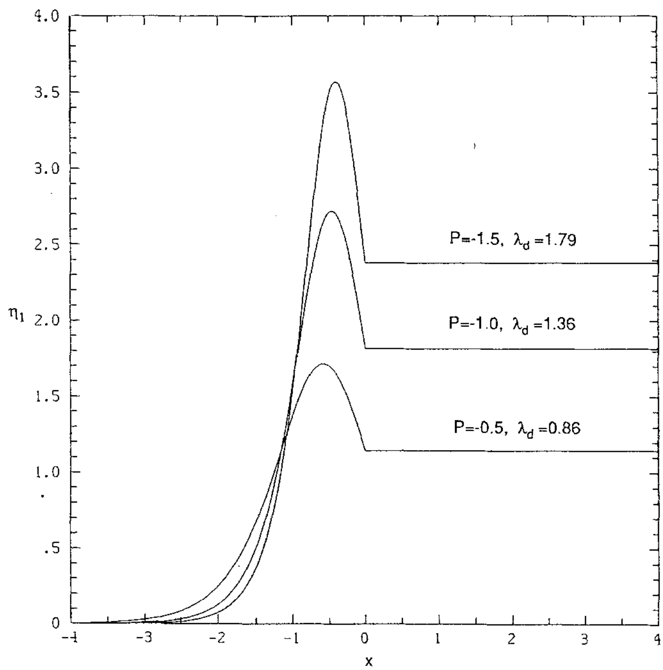

Figure 3(b)

Figure 3
Level-jump solutions (14) in a rectangular channel: $b = d = 1$, $\alpha = -\beta = -\frac{1}{6}$, $m_1 = -2$. a) $P > 0$ b) $P < 0$.

The bounded solution of the above problem is unique [11]. When $x < 0$, the solution vanishes identically.

$$\eta_1(x) \equiv 0 \quad \text{when } x \leq 0.$$

Therefore solving the problem (33)–(34) is equivalent to integrating the following initial value problem

$$\lambda\eta_1 + \alpha\eta_1^2 + \beta\eta_{1xx} = 0, \quad x > 0 \tag{35}$$

$$\eta_1(0+) = 0, \tag{36}$$

$$\eta_{1x}(0+) = -\frac{bP}{m_1}. \tag{37}$$

The first integral of the above gives

$$\frac{3\beta}{2\alpha}(\eta_{1x})^2 = -\eta_1^3 - \frac{3\lambda}{2\alpha}\eta_1^2 + \frac{3\beta}{2\alpha}\left(\frac{bP}{m_1}\right)^2 \equiv P(\eta_1), \quad x > 0, \tag{38}$$

$$\eta_1(0+) = 0. \tag{39}$$

In the above λ can be chosen to make $P(\eta_1)$ have three distinct real zeros, a double real zero, or only one real zero. Correspondingly, the problem (38)–(39) has a cnoidal wave solution, a wave free solution (hydraulic fall [4]), and an unbounded solution respectively [15, 16]. Let

$$\lambda_L = \left[3\frac{\alpha^2 b^2 P^2}{\beta m_1^2}\right]^{1/3} < 0. \tag{40}$$

Then $P(\eta_1)$ has three distinct real zeros, a double real zero, and only one real zero if $\lambda < \lambda_L$, $\lambda = \lambda_L$ and $\lambda > \lambda_L$ respectively.

Thus, (38)–(39) has

(i) A cnoidal wave solution when $\lambda < \lambda_L$,
(ii) a hydraulic fall solution when $\lambda = \lambda_L$,
(iii) no bounded solutions when $\lambda > \lambda_L$.

From (40), one can see that for the given geometry of a channel (α, β and b are determined), λ_L depends only on P. Comparing (23) and (40), we see that $|\lambda_L| > \lambda_c$.

When $\lambda < \lambda_L$, the cnoidal wave solution (38)–(39) can be expressed in terms of a Jacobian elliptic function

$$\eta_1(x) = \frac{\lambda}{\alpha}\left[\cos\left(\theta + \frac{4\pi}{3}\right) - \frac{1}{2} + \left(\cos\theta - \cos\left(\theta + \frac{4\pi}{2}\right)\right)\right.$$
$$\left.\cdot \mathrm{cn}^2\sqrt{\frac{\lambda}{6\beta}\left(\cos\theta - \cos\left(\theta + \frac{2\pi}{3}\right)\right)}(x - x_0)\right]. \tag{41}$$

The phase shift x_0 is in $[0, T]$ and is determined by $\eta_1(0+) = 0$, i.e.

$$\tfrac{1}{2} - \cos\left(\theta + \frac{4\pi}{3}\right)$$
$$= \left(\cos\theta - \cos\left(\theta + \frac{4\pi}{3}\right)\right) \mathrm{cn}^2\left(\sqrt{\frac{\lambda}{6\beta}\left(\cos\theta - \cos\left(\theta + \frac{2\pi}{3}\right)\right)}\, x_0\right).$$

Here T is the period of the cnoidal wave (41) and is given by

$$T = 2K(k^2) \Big/ \sqrt{\frac{\lambda}{6\beta}\left(\cos\theta - \cos\left(\theta + \frac{2\pi}{3}\right)\right)}. \tag{42}$$

The parameters θ and k^2 are

$$\theta = \tfrac{1}{3} \arccos\left[-1 + \frac{6\beta}{\lambda^3}\left(\frac{\alpha b P}{m_3}\right)^2\right] \le \frac{\pi}{3}, \tag{43}$$

$$k^2 = \frac{\cos\theta - \cos\left(\theta + \dfrac{4\pi}{3}\right)}{\cos\theta - \cos\left(\theta + \dfrac{2\pi}{3}\right)} \le 1.$$

$K(k^2)$ is the complete elliptic integral.

The closer λ is to λ_L, the larger is the period T of the cnoidal wave. When $\lambda \uparrow \lambda_L$, this period approaches infinity and the cnoidal wave solution becomes a wave free solution. This is the hydraulic fall [4, 11]. This conclusion can be easily derived from (30), and (42)–(43). When $\lambda = \lambda_L$, we have $\theta = 0$, $k^2 = 1$. Since $K(1) = \infty$, the period $T = \infty$ by (42). The solution (41) becomes

$$\eta_1(x) = (\lambda_L/\alpha)[-1 + (3/2)\mathrm{sech}^2\sqrt{\lambda_L/(4\beta)}(x - x_0)], \quad x > 0 \tag{44}$$

where x_0 is determined by $\eta_1(0+) = 0$, i.e.

$$x_0 = \sqrt{4\beta/\lambda_L}\ \mathrm{arc\,sech}\sqrt{2/3}. \tag{45}$$

The downstream depth is $H_D = (1 - \varepsilon\lambda_L/\alpha)H < H$. So the free surface falls to a lower level from the upstream higher level. Next we show that in a square channel the down stream flow is supercritical for such a hydraulic fall. Let U_D and H_D be the downstream velocity and depth. The conservation of mass flux yields

$$U_D H_D = (1 + \varepsilon\lambda_L + 0(\varepsilon^2))\sqrt{gH}H.$$

Then the downstream Froude number F_D is

$$F_D = U_D/\sqrt{gH_D}$$
$$= 1 - \varepsilon\lambda_L + 0(\varepsilon^2) > 1 \text{ (supercritical).}$$

Another limit is the case when $\lambda \to -\infty$. Then $\theta \approx \pi/3$, $k^2 \approx 0$, and $K(k^2) \approx K(0) = \pi/2$. Hence the period is $T = 2\pi/\sqrt{-6\lambda}$. The cnoidal waves

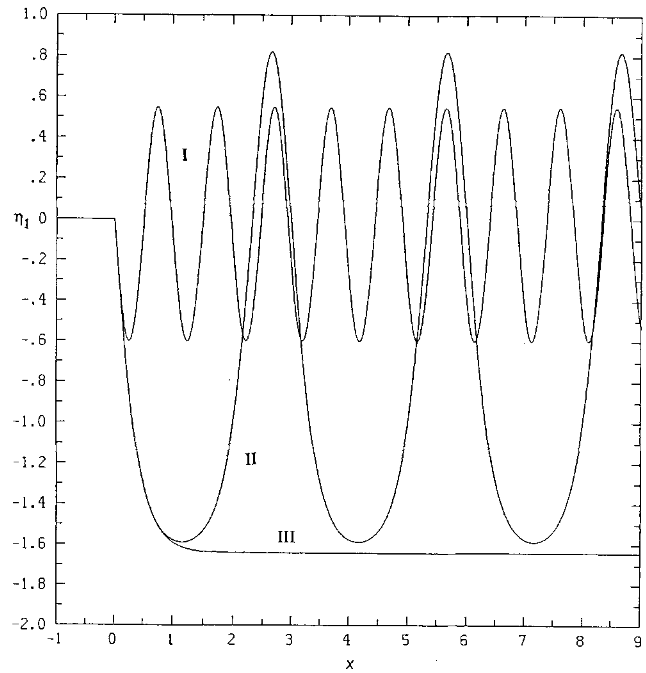

Figure 4
Profiles of three typical subcritical surface waves: sinusoidal wave (I), cnoidal wave (II) and hydraulic fall (III) for a triangular channel: $b = d = 1$, $\alpha = -\frac{5\sqrt{2}}{8}$, $\beta = -\frac{13\sqrt{2}}{192}$, $m_3 = 13/48$, $P = 1.0$, $\lambda = -4.0$ for I, $\lambda = -1.455$ for II, and $\lambda = \lambda_L = -1.451$ for III.

become approximately sinusoidal waves whose amplitudes approach zero as $\lambda \to -\infty$. The subcritical cnoidal waves, hydraulic falls and sinusoidal waves are shown in Figure 4 for triangular channel.

5. Concluding remarks

We have studied stationary long free surface waves of a perfect fluid in channels of arbitrary cross section. The upstream flow velocity is near critical, i.e. $u_0 = u_c + \varepsilon\lambda + O(\varepsilon^2)$. An external distributed pressure is applied on the free surface. The length of the support of the distributed pressure is very small compared with the wave length. If the free surface elevation η is written as $\eta(x, y, t) = \varepsilon\eta_1(x, t) + O(\varepsilon^2)$, then η_1 satisfies a forced K–dV equation. If $\eta_1(-\infty) = \eta_{1x}(-\infty) = \eta_{1xx}(-\infty) = 0$, then stationary solutions of the forced K–dV equation exist only when $\lambda \notin (\lambda_L, \lambda_c)$. Here λ_L and λ_c are given by (40) and (23) respectively. In the case of rectangular channel with $b = d = 1$, the interval (λ_L, λ_c) reduces to the transcritical range of Froude number first discovered by Miles [7].

For a given $\lambda > \lambda_c$, there are two cusped solitary wave solutions (see Figures 2c), d)). This is consistent with those results presented in [10]. From the bifurcation diagrams (Figures 2a)), we see that as P approaches zero, the lower solution is going to vanish and the upper solution is going to the free solitary wave. It is well known that a free solitary wave is stable and its amplitude is proportional to the upstream velocity. But in the case of positive forcing ($P > 0$), the solutions of the lower branch is inversely proportional to the upstream velocity. Hence we conjecture that this lower solitary wave solution is unstable. However, this intuitively reasonable conjecture has not yet been proved. Mathematically, this conjecture can be stated as follows: In the bifurcation diagram, if $(d/d\lambda)\|\eta_1\|_\infty > 0$ (<0), the corresponding solution is stable (unstable respectively), i.e.

Positive slope $\Leftrightarrow$ stable

Negative slope $\Leftrightarrow$ unstable

We refer this as *the slope stability theorem.*

When $\lambda \in (\lambda_L, \lambda_c)$, the forced $K-dV$ (4) does not have a stationary solution which satisfies $\eta_1(\pm\infty) = \eta_{1x}(\pm\infty) = \eta_{1xx}(\pm\infty) = 0$. Instead, according to the experimental and numerical results of Cole [6], Grimshaw and Smyth [19] and Wu [9] solitons are periodically generated at $x = 0$ and radiated upstream from some $\lambda \in (\lambda_L, \lambda_c)$.

Acknowledgements

The author is grateful for many extremely useful conservations with Professor M. C. Shen of University of Wisconsin-Madison. The research has been partly supported by the Climate System Research Program, Texas A&M University under Professor G. R. North and Natural Sciences and Engineering Research Council of Canada.

References

[1] D. M. Wu and T. Y. Wu, *Three-dimensional nonlinear long waves due to moving surface pressure*, In Proc. 14th Symp. Naval Hydrodyn., 103–129 (1982).
[2] L. K. Forbes and L. W. Schwartz, *Free surface flow over a semi-circular obstruction*, J. Fluid Mech. *114*, 299–314 (1982).
[3] J. M. Vanden-Broeck, *Free-surface flow over an obstruction in a channel*, Phys. Fluids *30*, 2315–2317 (1987).
[4] L. K. Forbes, *Critical free-surface flow over a semi-circular obstruction*, J. Engr. Math. *22*, 3–13 (1988).
[5] T. R. Akylas, *On the excitation of long nonlinear water waves by a moving pressure distribution*, J. Fluid Mech. *141*, 455–466 (1984).
[6] S. L. Cole, *Transient waves produced by flow past a bump*, Wave Motion *7*, 579–587 (1985).
[7] J. W. Miles, *Stationary, transcritical channel flow*, J. Fluid Mech. *162*, 489–499 (1986).

[8] C. C. Mei, *Radiation of solitons by slender bodies advancing in a shallow channel*, J. Fluid Mech. *162*, 53–67 (1986).
[9] T. Yao-tsu Wu, *Generation of upstream advancing solitons by moving disturbances*, J. Fluid Mech. *184*, 75–99 (1987).
[10] S. S. P. Shen, *Disturbed critical surface waves in a channel of arbitrary cross section*, J. Appl. Math. Phys. (ZAMP) *40*, 219–229 (1989).
[11] S. S. P. Shen and M. C. Shen, *A new equilibrium of subcritical flow over an obstruction in a channel of arbitrary cross section*, Eur. J. Mech. (B/Fluids) *9*, 59–74 (1990).
[12] R. C. Ertekin, W. C. Webster and J. V. Wehausen, *Waves caused by a moving disturbance in a shallow channel of finite depth*, J. Fluid Mech. *169*, 275–292 (1986).
[13] A. Patone and T. Warn, *The interaction of long, quasi-stationary baroclinic waves with topography*, J. Atmos. Sci. *39*, 1018–1025 (1982).
[14] A. S. Fokas and M. J. Ablowitz, *Forced nonlinear evolution equations and the inverse scattering transform*, Stud. Appl. Math. *80*, 253–272 (1989).
[15] G. B. Whitham, *Linear and Nonlinear Waves*, John Wiley & Sons, New York, Ch. 13, 1974.
[16] T. B. Benjamin and M. J. Lighthill, *On cnoidal waves and bores*, Proc. R. Soc. Lond. *A224*, 448–460 (1954).
[17] C. S. Yih, *Fluid Mechanics*, West River Press, Ann Arbor 1979.
[18] Y. H. Cai and M. C. Shen, *The development of a solitary wave in a channel of variable elliptic cross section*, Phys. Fluids *28*, 3252–2356 (1985).
[19] R. H. J. Grimshaw and N. Smyth, *Resonant flow of a stratified fluid over topography*, J. Fluid Mech. *169*, 429–464 (1986).

Abstract

Critical long surface waves forced by locally distributed external pressure applied on the free surface in channels of arbitrary cross section are studied in this paper. The fluid under consideration is inviscid and has constant density. The upstream flow is uniform and the upstream velocity is assumed to be near critical, i.e., $u_0 = u_c + \varepsilon\lambda + 0(\varepsilon^2)$, where $0 < \varepsilon \ll 1$ and u_c is the critical velocity determined by the geometry of the channel. The external pressure applied on the free surface as the forcing is $\varepsilon^2 P\delta(x)$. Then the first order perturbation of the free surface elevation satisfies a forced Korteweg–de Vries equation ($fK-dV$). It is shown in this paper that: (i) If $\lambda \geq \lambda_c = (3b^2P^2\alpha^2/(-4\beta m_1^2))^{1/3} > 0$ (supercritical), the stationary $fK-dV$ has two cusped solitary wave solutions; (ii) if $\lambda < \lambda_L = (3b^2P^2\alpha_2/\beta m_1^2)^{1/3} < 0$ (subcritical), the stationary $fK-dV$ has a downstream cnoidal wave solution; (iii) when $\lambda = \lambda_L$, the unique stationary solution of the $fK-dV$ is a wave free hydraulic fall; (iv) if $\lambda = \lambda_d = -\lambda_L$, the $fK-dV$ has a jump solution; and (v) if $\lambda_L < \lambda < \lambda_c$, the $fK-dV$ does not have stationary solutions. Some free surface profiles and bifurcation diagrams are presented.

(Received: November 30, 1989; revised: July 16, 1990)